



OPEN

UPLC/MS-based untargeted metabolomics reveals the changes of metabolites profile of *Salvia miltiorrhiza* bunge during Sweating processing

Mengyang Cao^{1,2}, Yingying Liu³, Weimin Jiang⁴, Xiaoxi Meng⁵, Wei Zhang¹, Weidong Chen¹, Daiyin Peng^{1,2,6} & Shihai Xing^{1,2,7}✉

Salvia miltiorrhiza has numerous compounds with extensive clinical application. "Sweating", a processing method of Traditional Chinese Medicine (TCM), results in great changes in pharmacology and pharmacodynamics. Previously, chromatogram of 10 characteristic metabolites in *S. miltiorrhiza* showed a significant difference after "Sweating". Due to the complexity of TCM, changes in metabolites should be investigated metabolome-wide after "Sweating". An untargeted UPLC/MS-based metabolomics was performed to discover metabolites profile variation of *S. miltiorrhiza* after "Sweating". Multivariate analysis was conducted to screen differential metabolites. Analysis indicated distinct differences between sweated and non-sweated samples. 10,108 substance peaks had been detected altogether, and 4759 metabolites had been identified from negative and positive ion model. 287 differential metabolites were screened including 112 up-regulated and 175 down-regulated and they belong to lipids and lipid-like molecules, and phenylpropanoid and polyketides. KEGG analysis showed the pathway of linoleic acid metabolism, and glyoxylate and dicarboxylate metabolism were mainly enriched. 31 and 49 identified metabolites were exclusively detected in SSM and NSSM, respectively, which mainly belong to carboxylic acids and derivatives, polyketides and fatty acyls. By mapping tanshinones and salvianolic acids to 4759 identified metabolites library, 23 characteristic metabolites had been identified, among which 11 metabolites changed most. We conclude that "Sweating" has significant effect on metabolites content and composition of *S. miltiorrhiza*.

Salvia miltiorrhiza Bunge, referred to as "Danshen" in China or "Tanshen" in Japan, which is an important species in *Salvia* genus with great medicinal values¹, was first recorded in *Shennong Bencaojing*, the earliest famous extant monograph of traditional Chinese pharmacology in China². The dry roots and rhizomes of *S. miltiorrhiza*, called Danshen, have been extensively used in the clinical treatments of many different diseases, such as coronary heart disease³, hyperlipidemia⁴, cerebrovascular disease⁵, Alzheimer's disease⁶, hypertension⁷, cancer⁸ and osteoporosis⁹.

Because Danshen has a broad prospect of clinical application, lots of effort has been made to investigate the main constituents and bioactive ingredients of Danshen¹⁰. The bioactive components of Danshen are mainly divided into fat-soluble tanshinones belonging to diterpene and water-soluble caffeic acid-derived salvianolic acids^{11,12}. Thus far, more than 40 tanshinones and over 50 salvianolic acids have been well isolated and identified

¹College of Pharmacy, Anhui University of Chinese Medicine, Room 405, Qianjiang Road No. 1, Yaohai District, Hefei 230012, Anhui Province, China. ²Institute of Traditional Chinese Medicine Resources Protection and Development, Anhui Academy of Chinese Medicine, Hefei 230012, China. ³College of Humanities and International Education Exchange, Anhui University of Chinese Medicine, Hefei 230012, China. ⁴College of Life Sciences and Environment, Hengyang Normal University, Hengyang 421008, Hunan, China. ⁵Department of Horticultural Science, University of Minnesota, Minneapolis, MN 55108, USA. ⁶Synergetic Innovation Center of Authentic Chinese Medicine Quality Improvement, Hefei 230038, China. ⁷Anhui Province Key Laboratory of Research and Development of Chinese Medicine, Hefei 230012, China. ✉email: xshshihai@163.com

from roots of *S. miltiorrhiza*. Tanshinones mainly include tanshinone I, tanshinone IIA (TsIIA), tanshinone IIB, cryptotanshinone and dihydrotanshinone I, and salvianolic acids mainly consist of salvianolic acid A (Sal A), salvianolic acid B (Sal B), lithospermic acid, danshensu, caffeic acid, and rosmarinic acid^{13,14}.

The initial processing of TCM is important and closely related to the quality of TCM's products²². The initial processing of medicinal materials is from the harvest of medicinal parts to the formation of commercial medicinal materials, such as preliminary treatment and drying²³. At present, initial processing methods mainly include slicing while the herbs are still fresh, drying and packing²⁴. Medicinal materials are formed through the above-mentioned processing, during which physical and chemical changes take place, such as the removal of non-medicinal parts, the maximum retention of active substances, the reduction of toxic components, and the mutual transformation of chemical components²³. The medicinal materials forming during initial processing are the raw materials of Chinese herbal slices. Their quality directly affects the quality of Chinese herbal slices, and then affects the clinical curative effect of TCM²⁵.

"Sweating" is the main initial processing method for Danshen roughly as follows: the fresh roots of *S. miltiorrhiza* are piled up and covered to produce heat and emit moisture to the surface of the materials²⁶. "Sweating" is beneficial not only to the drying of herbs, but also to regulate and promote the enzyme system and microbial community activity in herbs tissues, and accelerate the process of biotransformation and chemical transformation of primary and secondary metabolites, which directly affects the quality of medicinal materials²⁷. Pharmacological activities of medicinal materials can be changed by "Sweating". Some related pharmacodynamic studies have shown that the antioxidant activity²⁸, brain protective effect, and myocardial protective effect of "Sweating" *S. miltiorrhiza* (SSM) are stronger than those of non-sweating *S. miltiorrhiza* (NSSM)²⁹. Cocktail probed drug method has been used to study the effects of SSM and NSSM on CYP450 enzyme activity in rats. The result has shown that there are significant differences in effects of SSM and NSSM on CYP450 enzyme activity in rats²⁸. The unique pharmacology and efficacy of SSM is a reflection of hundreds of bioactive compounds rather than a single or several ones. In addition, the various activities of components in Danshen are considered responsible for the therapeutic effects of Danshen³⁰. Therefore, it is necessary to study the changes of the composition and content of chemical components in roots of *S. miltiorrhiza* after "Sweating". However, due to the complexity of Traditional Chinese Medicine (TCM), it's far from enough to be merely focused on several main bioactive components in TCM but ignore the whole changes of the metabolites³¹, and it's difficult to comprehensively and accurately investigate the effect of "Sweating" on the chemical composition of Danshen by only determining some main components. Consequently, studies of the overall chemicals profile of "Sweating" on Danshen are necessary to better understand the mechanism of "Sweating".

Untargeted metabolomics is a valuable technique for comprehensive analysis and comparison of end-product metabolites in the process of cell regulatory processes, and their levels can be considered as the ultimate response of the biological system to changes in endogenous and/or exogenous factors³². The LC-MS method is a useful tool to analyze the components of herbal medicine, which provides efficient visualization and identification of the metabolites³³. It shows metabolite selectivity and sensitivity to targeted analysis, and detects low concentration compounds that may not be detected by other methods³⁴. In this study, we used *S. miltiorrhiza* without "Sweating" (NSSM) and Danshen just after "Sweating" (SSM) as experimental materials. UPLC-MS-based metabolomics combined with multivariate statistical analysis was applied to reveal the metabolic profile differences between NSSM and SSM so as to investigate the effect of "Sweating" on the global metabolic profile of Danshen.

The difference of components between SSM and NSSM materials in this study merely comes from "Sweating" process without long-term storage leading to complex components loss, with which may result in non-unique difference. Additionally, we compared the changes of some main characteristic bioactive components in Danshen before and after "Sweating" to specifically reveal the effect of "Sweating". The results gave a deeper insight into the mechanism behind "Sweating" of Danshen and a better explanation of the scientific connotation of "Sweating".

Results and discussion

Identification of global metabolite profiling. Methanol extracts from the roots of SSMs and NSSMs were measured by a UPLC system fitted with Q-Exactive quadrupole-Orbitrap mass spectrometer (Thermo Fisher Scientific, Waltham, MA, USA) to investigate the metabolic changes during the "Sweating" processing and identify critical metabolites responsible for metabolomics variation by "Sweating" processing.

Typical total ions current chromatograms (TICs) of SSM and NSSM is shown in Fig. 1a (ESI⁺) and Fig. 1b (ESI⁻), respectively. L-2-chlorophenylalanine (C₉H₁₀ClNO₂) with RT (retention time) at 2.514 min and LPC (17:0) (C₂₅H₅₂NO₇P) with RT 6.430 min was added to the extracts as two internal standards (L-2-chlorophenylalanine with mass number 200.0478, 0.3 mg/mL; Lyso PC17: 0 with mass number 510.3481, 0.3 mg/mL). Metabolites in Danshen samples were identified according to internal standards and metabolomics databases of the Human Metabolome Database (HMDB), Lipidmaps (v 2.3) and METLIN by the software of Progenesis QI V2.3. A total of 10,108 substance peaks were detected by UPLC-MS in the samples of SSM and NSSM, among which 4759 metabolites were identified including 2241 metabolites from negative ion model (ESI⁻) and 2518 metabolites from positive ion mode (ESI⁺), respectively (Fig. 1c, Supplementary Table S1).

Multivariate analysis of identified metabolites. Unsupervised principal components analysis (PCA) was carried out on the detected 10,108 substance peaks, QC samples and the two kinds of samples SSM and NSSM were classified into different metabolite profile with a significance of 0.05 by PCA, showing good stability and repeatability of the LC/MS detection (Fig. 2a). In order to visualize the metabolites differences between experimental samples and QC samples, and eliminate the effects of quantity on pattern recognition, hierarchical cluster analysis (HCA) and a log₁₀ transformation of peak areas for each metabolite were performed. Samples

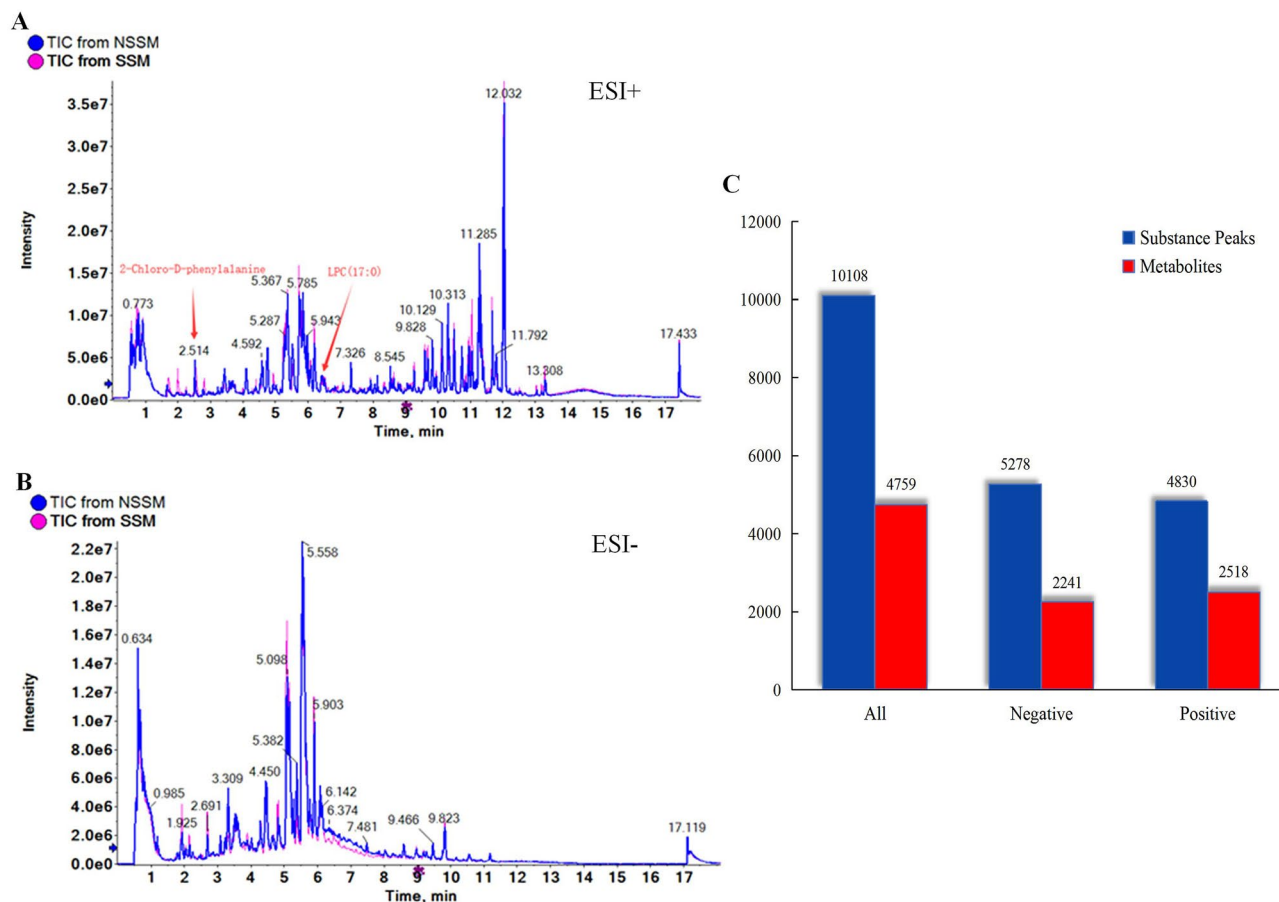


Figure 1. Total ions chromatograms (TICs) of methanol extracts from SSM and NSSM and global metabolites identified. **a** TICs of positive electrospray ionization (ESI⁺), and arrows indicate inner standards, **b** TICs of negative ESI (ESI⁻), **c** The number of substance peaks determined and metabolites identified.

of SSM, NSSM and QC were merged into independent cluster (Supplementary Figure S1). Thus, PCA combined with HCA indicates that samples of SSM and NSSM had remarkably differential metabolic profiles.

The supervised method, partial least square discrimination analysis (PLS-DA) was also applied to investigate the metabolites difference between SSM and NSSM samples (Fig. 2b). The calculated R^2 value of PCA and Q value of PLS-DA are shown in Fig. 2, and the values indicated that there was statistically significant difference between SSM and NSSM. The orthogonal PLS-DA (OPLS-DA), another supervised method, was used to highlight the quantitative variation in the metabolites between two samples, and good model quality was also shown by the value of R^2X and Q^2 (Fig. 2c). The OPLS-DA score of each sample in this figure once again showed that there was significant difference among them ($p < 0.5$). The cross-validation with 200 permutation tests indicated that this OPLS-DA model was reliable, with intercepts of R^2 and Q^2 equal to 0.654 and -0.516 , respectively (Fig. 2d).

Screening and classification of the differential metabolites. To visualize the result of fold change analysis of 10,108 substance peaks, a volcano plot was drawn by transferring the fold change (FC) value of each substance peak to \log_2 (FC), and transferring the P value ($P = 0.05$) of Student's t test to $-\log_{10}(P \text{ value})$. Among all of the differential metabolites, upregulated metabolites (SSM compared with NSSM) were symbolized with red dots gathered into a group and downregulated metabolites with blue dots gathered into a group (Fig. 3a). As shown in the volcano plot, there were obvious differences in metabolites between the two samples.

To identify differential metabolites between samples, a fold change ≥ 1.6 (up-regulated) or ≤ 0.625 (down-regulated) in SSM compared to NSSM, and these metabolites were screened using a variable importance in projection (VIP) value ($VIP \geq 1.0$) from the OPLS-DA model. A total of 287 differential metabolites had been identified from total 4759 identified metabolites between SSM and NSSM by VIP and FC value, containing 130 and 157 metabolites from the positive and negative model, respectively (Fig. 3b, Supplementary Table S2).

Of these differential metabolites, 112 metabolites were up-regulated and 175 metabolites were down-regulated in SSM compared with NSSM. The majority of differential metabolites were lipids and lipid-like molecules, phenylpropanoid and polyketides, benzenoids, organic acids and derivatives, organic oxygen compounds, and there were 30 unclassified chemicals (Fig. 4a). These results showed the process of "Sweating" notably changed the metabolic profile of Danshen.

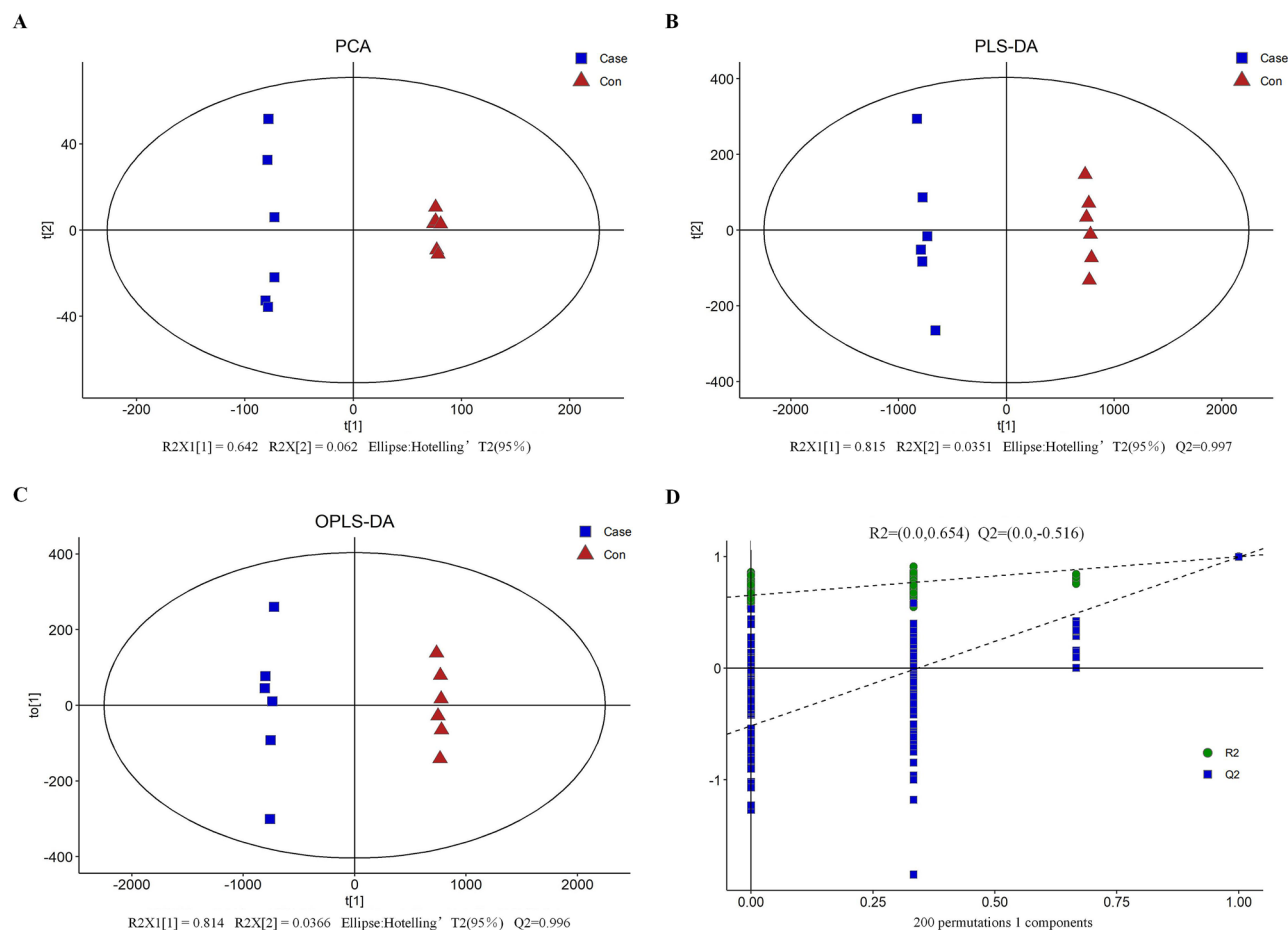


Figure 2. Model of multivariate analysis and its cross validation. **a** Principal components analysis (PCA), **b** partial least square discrimination analysis (PLS-DA), **c** orthogonal PLS-DA (OPLS-DA), **d** response permutation testing of the model predicted by OPLS-DA. R2X (cum): cumulative interpretation rate in X direction, R2Y (cum): cumulative interpretation rate in Y direction, Q2 (cum): cumulative forecast rate of model, R2 and Q2: parameters of response sequencing test, used to measure whether the model is over fitted.

Emerging literature has indicated that lipids and lipid-like molecules have less anti-inflammatory properties, higher antioxidant effects, immunomodulatory effect, and decrease the risk of cholestasis, and improve clinical outcomes of certain subgroups of patients³⁵. Research has shown that phenylpropanoid and polyketides possess anticarcinogenic, anti-inflammatory, neuroprotective, immunomodulatory, antihypertensive, and metabolic effects³⁶. Benzenoids have the effect on anti-inflammatory³⁷. All of these results indicate that changes in these differential metabolites are responsible for great change in Danshen's pharmacological effects during the process of "Sweating".

KEGG classification and enrichment analysis of differential metabolites. We mapped the 287 differential metabolites to the KEGG (Kyoto Encyclopedia of Genes and Genomes) database, looking first at information about pathways³⁸. Our result showed that 51 metabolites mapped to "metabolism" and they had KEGG ID. Subsequently, KEGG pathway enrichment analysis was conducted to identify differences in metabolic pathway between SSM and NSSM samples. 19 metabolites had been found enriched in 30 KEGG pathways (Supplementary Table 3). By calculating the $-\lg(P\text{-value})$ of each pathway, linoleic acid metabolism was the most enriched pathway, glyoxylate and dicarboxylate metabolism and phenylpropanoid biosynthesis were also the main enriched pathways (Fig. 4b).

Previous study indicated that linoleic acid and related metabolic pathways are associated with bone mineral density³⁹. Linoleic acid help to protect liver safety in obese and overweight women and fight against mortality^{40,41}. Study also found biomarkers of *S. miltiorrhiza* that can improve hemorheological disorder and vascular endothelial function of microcirculation dysfunction rats are mainly related to linoleic acid metabolism, glutathione metabolism, and glyoxylate and dicarboxylate metabolism etc. All of the research indicated that changes in the core metabolites and their corresponding pathways culminate in improvement on pharmacological function of Danshen after "Sweating".

Top 50 differential metabolites analysis. Among these 297 differential metabolites, those differential metabolites in top 50 VIP value were collected. Ranking these metabolites by FC calculated from data matrix,

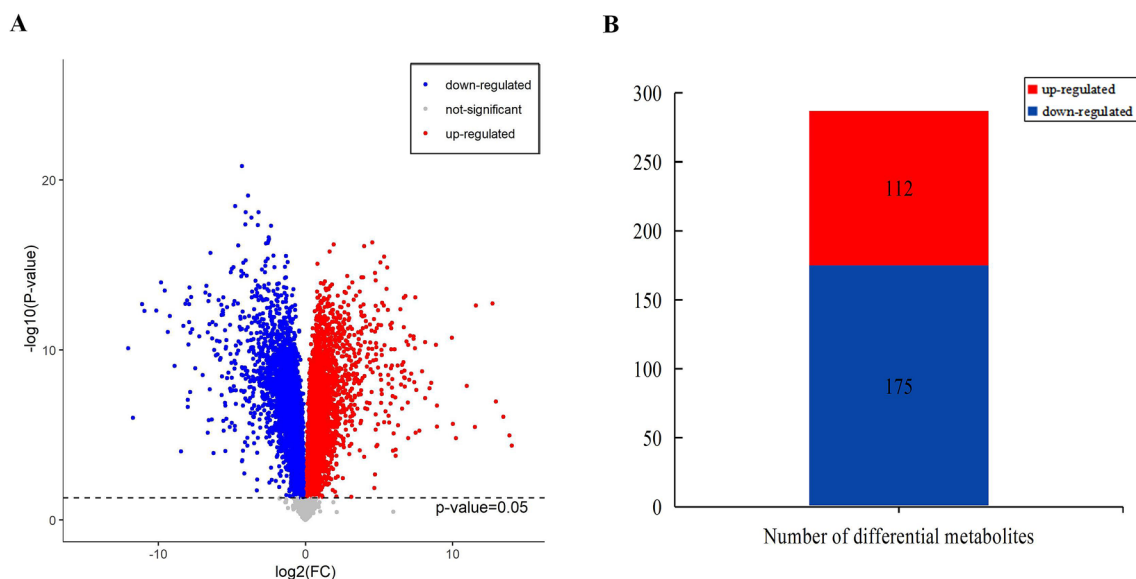


Figure 3. Differentially accumulating metabolites between SSM and NSSM. **a** Differential gene volcano plot of the 4759 metabolites identified. Differential metabolites were defined as metabolites with fold change ≥ 1.6 or ≤ 0.625 in SSM compared with NSSM. A threshold of VIP > 1.0 was used to separate differential metabolites from not-significantly differential metabolites, **b** number of differential metabolites between SSM and NSSM.

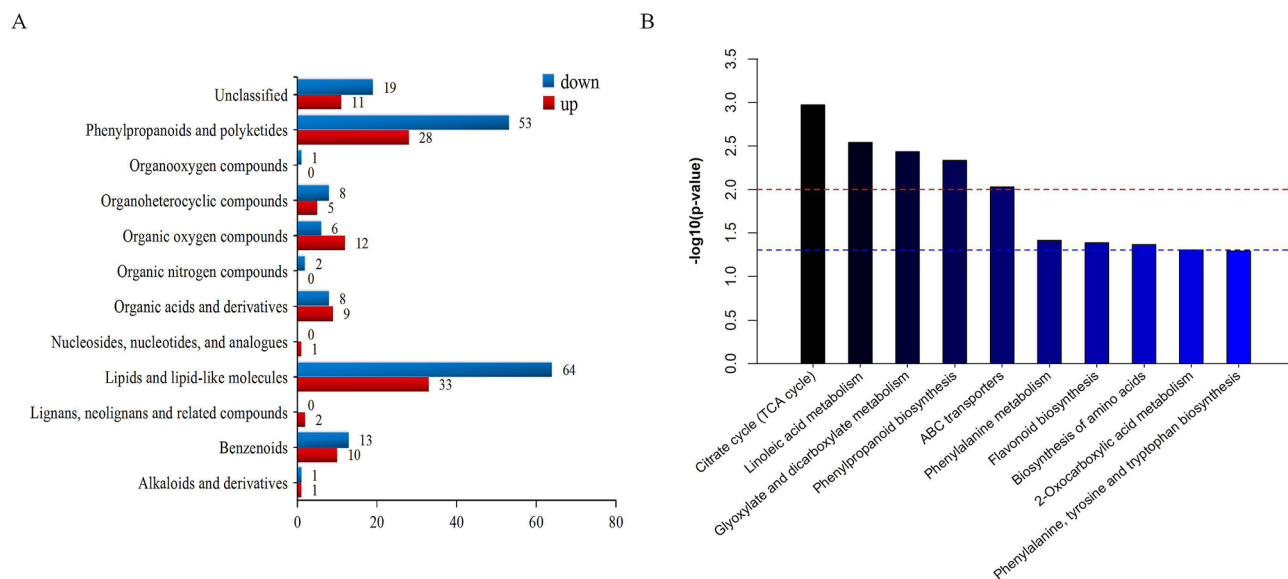


Figure 4. Classification of differential metabolites and pathways enrichment. **a** Classification of differential metabolites, **b** top 10 enriched pathways, red line dotted line shows P -value is 0.01 and blue dotted line shows P -value is 0.05.

it showed that the content of indoleacrylic acid with the highest content by “Sweating” was at 7.54 folds, while the content of psoromic acid was only about 5% compared to NSSM (Supplementary Table S4). A heatmap was drawn using the top 50 differential metabolites, there’s significant difference between SSM and NSSM materials (Fig. 5). The conclusion can be reached that there was a marked change in the content of compounds during Danshen “Sweating” processing.

Indoleacrylic acid (IAA), as a plant hormone, was found to have the function to promote anti-inflammatory responses and therapeutic benefits⁴², and previous study has shown that IAA can inhibit tumor cell invasion, migration and cell proliferation in a dose-independent manner⁴³. It was reported that psoromic acid has anti-oxidant and cardiovascular protective effects⁴⁴. These top differential metabolites have their own effects and they work together to change the pharmacological activity of *Salvia miltiorrhiza*.

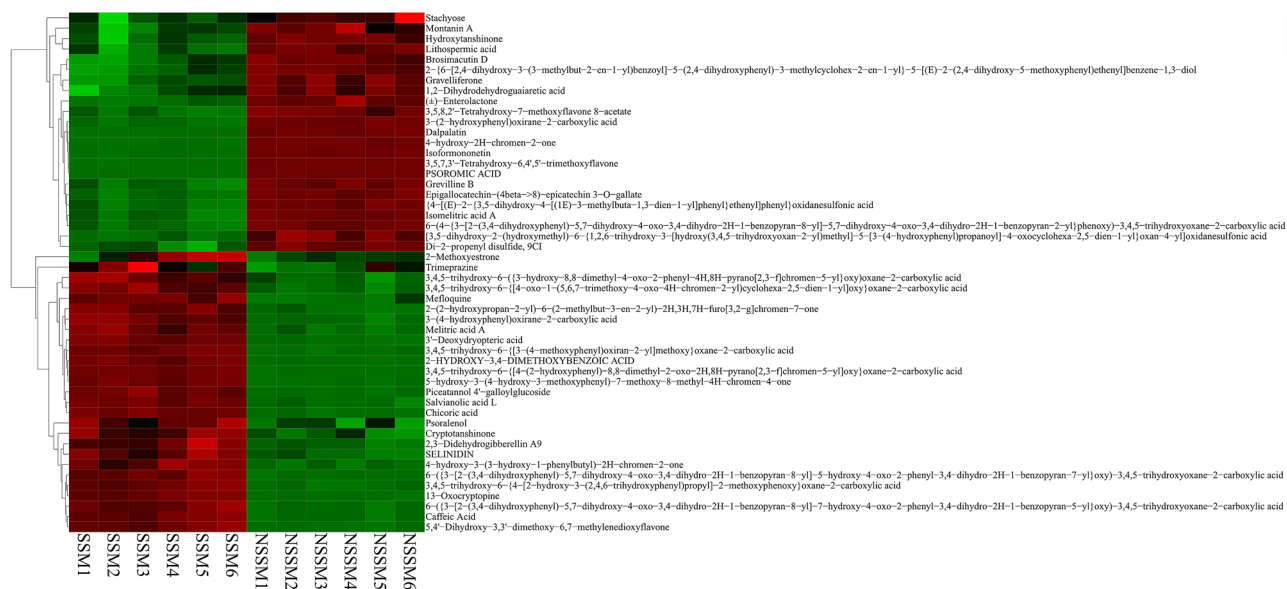


Figure 5. Heatmap of top 50 differential metabolites.

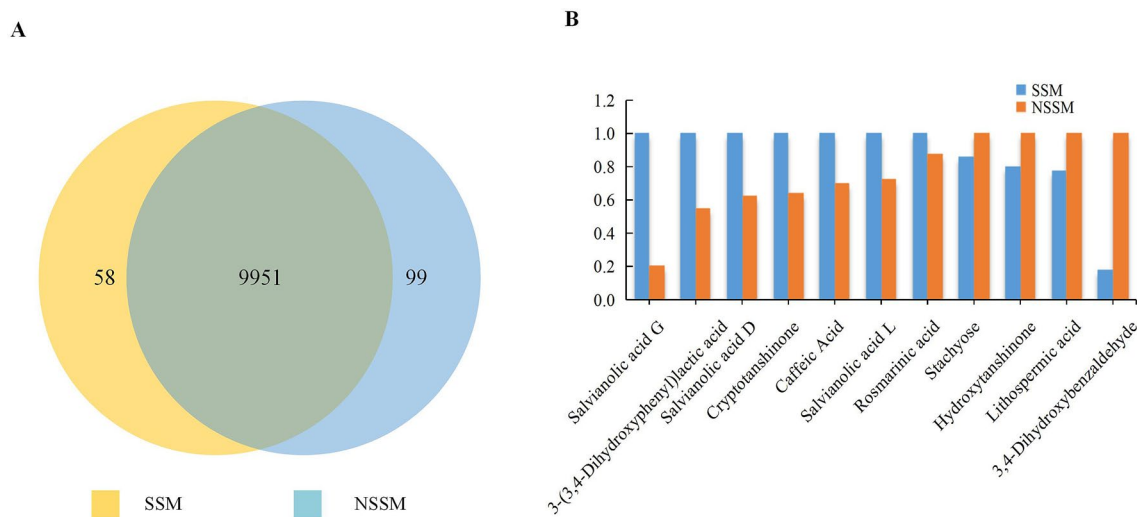


Figure 6. Comparison of differential and characteristic metabolites. **a** Venn diagram shows newly formed and vanished compounds after “Sweating”, **b** the content of differential characteristic metabolites in SSM and NSSM (the contents of each higher one convert to 1.0).

Newly generated and disappeared compounds. By comparing the sum of fragments ion strength of each substance peak, 58 substance peaks only emerged in SSM, among which 31 metabolites identified, including 19 from positive ion models (ESI⁺) and 12 from negative ion models (ESI⁻). 99 substance peaks were exclusively determined in NSSM with 49 metabolites identified, which contained 27 and 22 differential metabolites from ESI⁺ and ESI⁻, respectively (Fig. 6a, Supplementary Table 5). Among these 80 identified (31 in SSM and 49 in NSSM) exclusive metabolites, 20, 9, 6, 4, 4, 3 of them belonged to carboxylic acids and derivatives, polyketides, fatty acyls, flavonoids, prenol lipids, and benzene and substituted derivatives, respectively.

Characteristic Metabolites analysis by “Sweating”. Tanshinones and Salvianolic acids are the two kinds of characteristic bioactive compounds possessing magnificent bioactivities in Danshen. In this untargeted metabolomic study, a total of 23 specific compounds of Tanshinones and Salvianolic acids had been detected (Supplementary Table 6), and there was significant difference in content of 11 of them. And among these 11 characteristic differential metabolites, 7 metabolites content increased while 4 decreased in SSM compared with NSSM. In addition, there was the largest increase in the Salvianolic acid G content while the greatest reduction in the 3, 4-Dihydroxybenzaldehyde content of SSM compared to NSSM. (Fig. 6b). Correlating our previous study on Chromatographic Fingerprint of 10 target characteristic metabolites⁴⁵, we can come to the conclusion that there was a change in most of Tanshinones and Salvianolic acids content after “Sweating”. We suggest that a

transcriptomic (We had confirmed there was no degradation in total RNA after “Sweating”) or a proteomic study should be performed to investigate the change in genes or enzymes of Danshen during “Sweating” processing to explain the change of metabolites content of SSM.

Conclusions

Origin processing of “Sweating” has a significant effect on the metabolites content and composition of *S. miltiorrhiza*. There are 287 differential metabolites between sweated and non-sweated *S. miltiorrhiza* with 112 up-regulated and 175 down-regulated, and they mainly belong to lipids and lipid-like molecules, phenylpropanoid and polyketides, and Benzenoids. And these differential metabolites are mainly enriched in the pathway of linoleic acid metabolism, glyoxylate and dicarboxylate metabolism and phenylpropanoid biosynthesis. Total of 80 metabolites exclusively detected mainly belong to carboxylic acids and derivatives, polyketides, fatty acyls and flavonoids. Among them, 31 and 49 are detected in SSM and NSSM, respectively. A total of 23 metabolites that belong to tanshinones and salvianolic acids had been identified, and 11 metabolites content was changed significantly after “Sweating”.

Materials and methods

Chemicals and plant materials. Plants of *S. miltiorrhiza* Bunge were cultivated in National Breeding Base of Seeds and Seedlings of Medical Herbs for Essential Drugs in Anhui University of Chinese Medicine, Hefei, China.

Methanol, formic acid, water for LC/MS analysis and acetonitrile were all purchased from CNW Technologies GmbH (Düsseldorf, Germany). L-murine-2-chlorophenylalanine was obtained from Shanghai Hengchuang Bio-technology Co., Ltd. (Shanghai, China). LysoPC17: 0 was purchased from Avanti Company of the United States, and all of the chemicals and solvents were analytical or HPLC grade.

“Sweating” processing of plant materials. The same batch of *S. miltiorrhiza* was with all kinds of size collected, washed thoroughly and put in an open, clean, dry and cool place, so as to avoid overstocking during the process of natural water loss, preventing heat production. Then, reed heads were removed from the roots and picked over ones with uniform thickness and randomly divided them into two groups. One group (SSM) was processed by “Sweating”, and the other group (NSSM) was unprocessed and directly stored at $-80\text{ }^{\circ}\text{C}$. The steps of “Sweating” processing which are screened by modifying report from Liang et al. are as follows⁴⁶: More than 100 kg fresh roots with different sizes were piled up for seven days and covered with a sack to produce heat so as to make the internal moisture of root tissues spread outward in an open place. In order to make the whole roots sweat evenly, the roots were spread out for a night and then covered with sack every two days. When the internal sections of the roots turned purplish red, end “Sweating” and gather them up. Six independent sample pairs were collected from two groups and each sample pair of the same size were ground into powder after being lyophilized in a speed vacuum and sieving with 50 order mesh were stored at $-80\text{ }^{\circ}\text{C}$.

Sample preparation. The powdery samples (80 mg) after being precisely weighed were transferred to 1.5 mL Eppendorf tubes, and two small steel balls were added to each tube. Two internal standards 17:0 Lyso PC (1-heptadecanoyl-sn-glycero-3-phosphocholine), 0.01 mg/mL; (20 μL each) (L-2-chlorophenylalanine), 0.3 mg/mL, both of them were prepared with methanol and 1 mL mixture of methanol and water (3/7, v/v) were added to each sample, and the samples were pre-cooled at $-20\text{ }^{\circ}\text{C}$ for 2 min. Then the samples were ground at 60 Hz for 2 min, and stood under ultrasonication at ambient temperature for 30 min, and placed at $-20\text{ }^{\circ}\text{C}$ in refrigerator for 20 min. Samples were centrifuged at a speed of 13,000 rpm, $4\text{ }^{\circ}\text{C}$ for 10 min. 300 μL of supernatant in a brown glass vial was dried in a freeze concentration centrifugal dryer, and then added 400 μL mixture of methanol and water (1/4, v/v) to each sample, vortex for 30 s, and ultrasonicated for 2 min. Samples were centrifuged again at 13,000 rpm, $4\text{ }^{\circ}\text{C}$ for 10 min. The supernatants (about 150 μL) from each tube were collected using crystal syringes, filtered through microfilters at 0.22 μm and transferred to LC vials, and stored at $-80\text{ }^{\circ}\text{C}$ for LC–MS analysis. QC samples were prepared by mixing aliquots of 6 SSM and 6 NSSM to be a pooled sample, and used to balance the chromatography-mass spectrometer system.

LC/MS-based metabolomics analysis. A Dionex Ultimate 3000 RS UHPLC system fitted with Q-Exactive quadrupole-Orbitrap mass spectrometer equipped with heated electro-spray ionization⁴⁷ source (Thermo Fisher Scientific, Waltham, MA, USA) was used to analyze the metabolic profiling in both ESI positive and ESI negative ion modes. An ACQUITY UPLC BEH C18 column (1.7 μm , $2.1 \times 100\text{ mm}$) was employed in detecting both positive and negative modes. The binary gradient elution system consisted of (A) 0.1% (v/v) formic acid dissolved in water and (B) 0.1% formic acid (v/v) dissolved in acetonitrile and separation was achieved using the following gradient: 0 min, 5% B; 1.5 min, 5% B; 3 min, 30% B; 7 min, 60% B; 9 min, 90% B; 11 min, 100% B; 13 min, 100% B; 13.2 min, 5% B; 16 min, 5% B. The flow rate was at 0.35 mL/min and column temperature was at $40\text{ }^{\circ}\text{C}$. All the samples were kept at $4\text{ }^{\circ}\text{C}$ during the detection, the injection volume was at 5 μL each time, and the mass range was from m/z 100 to 1000. The resolution was set at 70,000 for the full MS scans and 17,500 for HCD MS/MS scans, and the Collision energy was set at 10, 20 and 40 eV. The mass spectrometer operated as follows: spray voltage, 3500 V at negative and positive mode; capillary temperature, $320\text{ }^{\circ}\text{C}$; sheath gas flow rate, 40 arbitrary units; auxiliary gas flow rate, 10 arbitrary units.

The QCs were injected at regular intervals (every 6 samples) throughout the analytical run to provide a set of data from which repeatability can be assessed, and were used to evaluate the stability of the mass spectrometer system during samples detection.

Data reduction and multivariate data analysis. The acquired LC–MS raw data were filtered by the software of Progenesis QI v2.3 (Nonlinear Dynamics, Newcastle, UK) through steps of baseline filtering, peak recognition, integration, retention time correction, peak alignment and normalization, and using the following parameters. Precursor tolerance was set at 5 ppm, product tolerance was set at 10 ppm, product ion threshold was set at 5%, and retention time (RT) tolerance was set at 0.02 min. Internal standard detection parameters were deselected for peak RT alignment, isotopic peaks were excluded for analysis, and noise elimination level was set at 10.00, minimum intensity was set to 15% of base peak intensity. The Excel file was obtained with three dimensions data sets including *m/z* (mass-to-charge ratio), peak RT (retention time) and peak intensities, and RT–*m/z* pairs were used as the identifier for each ion. The internal standard was used for data QC (reproducibility)⁴⁸.

Metabolites were identified by the Progenesis QI Data Processing Software (version 2.3, <https://www.nonlinear.com/progenesis/qi/>)⁴⁹ based on precise mass number, secondary fragments and isotope distribution, and qualitative by mapping on the Human Metabolome Database (HMDB), Lipidmaps (v 2.3) and METLIN database⁵⁰.

For the extracted data, delete the ion peaks whose missing values (ion intensity = 0) is more than 50% in the group, and replace the 0 value with the half of the minimum value, and screen the qualitative compounds according to the score of the qualitative results of the compounds. The screening standard is 30 points (Full score 60 points), and if the score is lower than 30 points, the qualitative results are deemed to be inaccurate and deleted. Finally, the positive and negative data were combined to get a combined data matrix table which contained all the information extracted from the original data, and was imported into R ropls package. Principle component analysis (PCA) and (orthogonal) partial least-squares-discriminant analysis (O)PLS-DA were carried out to visualize the metabolic alterations between sweating and non-sweating groups, after mean centering (Ctr) and Pareto variance⁵¹ scaling, respectively. The Hotelling's T2 region, shown as an ellipse in score plots of the models, defines the 95% confidence interval of the modeled variation. Variable importance in the projection (VIP) ranks the overall contribution of each variable to the OPLS-DA model, and those variables with VIP ≥ 1.0 are considered relevant for group discrimination⁵².

In this study, the default 7-round cross-validation and 200 times of response permutation testing (RPT) was applied with 1/seventh of the samples being excluded from the mathematical model in each round, in order to review the model quality and guard against over-fitting. The differential metabolites were selected on the basis of the combination of a statistically significant threshold of variable influence on projection (VIP) values obtained from the OPLS-DA model, P values from a two-tailed Student's t test on the normalized peak areas and the adjusting P value for correcting was obtained by Benjamini & Hochberg method, and fold change (FC) value SSM verse NSSM, where metabolites with VIP values ≥ 1.0 and p values < 0.05 were considered as differential metabolites. While calculating FC values, if the datum displaying the content of metabolite is zero, it would be changed by the half of the minimal corresponding value in the table of data matrix (2.5E-06)⁴⁸.

Univariate statistical analysis and differential metabolites visualization. The experimental data obtained in the present study is expressed as the mean ± standard deviation (SD) of six independent biological replicates, and the significance level of the metabolites between groups was calculated by one-way analysis of variance with Student's t test and fold change analysis using GraphPad Prism 7.00 software⁵³.

The volcano plot was used to visualize the P value from student's t test and the fold change (FC) value, which is conducive to screening differential metabolites, as shown in the figure with three different colors (red, blue and gray) to represent significantly up-regulated, down-regulated and non-significant differential metabolites in the experimental group.

KEGG pathway analysis of differential metabolites. Mapping the differential metabolites to KEGG data to look for their KEGG ID and the pathway they belonged to, then counting the number of metabolites enriched in corresponding pathway. The $-\lg(P\text{-value})$ was used to measure whether the pathway enriched or not, and the pathway was considered as enriched pathway when $P\text{-value} \leq 0.05$ ⁵⁰.

$$p = 1 - \sum_{i=0}^{m-1} \frac{\binom{M}{i} \binom{N-M}{n-i}}{\binom{m}{n}}$$

N: The number of total metabolites, n: The number of differential metabolites, M: Number of metabolites in specific pathway, m: Number of differential metabolites in specific pathway.

Data availability

The datasets generated during the current study are available in the Baidu Cloud repository: <https://pan.baidu.com/s/169-IDR72hzC6CvS0b537fA>. Access code: bb71.

Received: 11 August 2020; Accepted: 29 October 2020

Published online: 11 November 2020

References

1. Su, C. Y., Ming, Q. L., Rahman, K., Han, T. & Qin, L. P. *Salvia miltiorrhiza*: Traditional medicinal uses, chemistry, and pharmacology. *Chin. J. Nat. Med.* **13**, 163–182 (2015).
2. Jiang, Z., Gao, W. & Huang, L. Tanshinones, critical pharmacological components in *Salvia miltiorrhiza*. *Front. Pharmacol.* **10**, 202 (2019).

3. Huo, M., Wang, Z., Wu, D., Zhang, Y. & Qiao, Y. Using coexpression protein interaction network analysis to identify mechanisms of danshensu affecting patients with coronary heart disease. *Int. J. Mol. Sci.* **18**, 2017 (2017).
4. Cheung, D. W. *et al.* Evaluating efficacy and safety of combination medication of atorvastatin and a herbal formula containing Salvia miltiorrhiza and Pueraria lobata on hyperlipidemia. *Phytotherapy Res.* **31**, 1579–1589 (2017).
5. Shi, M. *et al.* Increased accumulation of the cardio-cerebrovascular disease treatment drug tanshinone in Salvia miltiorrhiza hairy roots by the enzymes 3-hydroxy-3-methylglutaryl CoA reductase and 1-deoxy-D-xylulose 5-phosphate reductoisomerase. *Funct. Integr. Genomics* **14**, 603–615 (2014).
6. Zhang, X. Z., Qian, S. S., Zhang, Y. J. & Wang, R. Q. Salvia miltiorrhiza: a source for anti-Alzheimer's disease drugs. *Pharm. Biol.* **54**, 18–24 (2016).
7. Yang, T. Y., Wei, J. C., Lee, M. Y., Chen, C. M. & Ueng, K. C. A randomized, double-blind, placebo-controlled study to evaluate the efficacy and tolerability of Fufang Danshen (Salvia miltiorrhiza) as add-on antihypertensive therapy in Taiwanese patients with uncontrolled hypertension. *Phytother. Res.* **26**, 291–298 (2012).
8. Jiang, G. *et al.* Anti-tumor and chemosensitization effects of Cryptotanshinone extracted from Salvia miltiorrhiza Bge on ovarian cancer cells in vitro. *J. Ethnopharmacol.* **205**, 33–40 (2017).
9. Cui, L. *et al.* Salvianolic acid B prevents bone loss in prednisone-treated rats through stimulation of osteogenesis and bone marrow angiogenesis. *PLoS ONE* **7**, e34647 (2012).
10. Wu, Y. B. *et al.* Constituents from Salvia species and their biological activities. *Chem. Rev.* **112**, 5967–6026 (2012).
11. Li, Z. M., Xu, S. W. & Liu, P. Q. Salvia miltiorrhizaBurge (Danshen): a golden herbal medicine in cardiovascular therapeutics. *Acta Pharmacol. Sin.* **39**, 802–824 (2018).
12. Chen, X., Guo, J., Bao, J., Lu, J. & Wang, Y. The anticancer properties of Salvia miltiorrhiza Bunge (Danshen): a systematic review. *Med. Res. Rev.* **34**, 768–794 (2014).
13. Shi, M., Huang, F., Deng, C., Wang, Y. & Kai, G. Bioactivities, biosynthesis and biotechnological production of phenolic acids in Salvia miltiorrhiza. *Crit. Rev. Food Sci. Nutr.* **59**, 953–964 (2019).
14. Dong, Y., Morris-Natschke, S. L. & Lee, K. H. Biosynthesis, total syntheses, and antitumor activity of tanshinones and their analogs as potential therapeutic agents. *Nat. Prod. Rep.* **28**, 529–542 (2011).
15. Gao, H. *et al.* Simultaneous purification of dihydrotanshinone, tanshinone I, cryptotanshinone, and tanshinone IIA from Salvia miltiorrhiza and their anti-inflammatory activities investigation. *Sci. Rep.* **8**, 8460 (2018).
16. Fu, L. *et al.* The anticancer properties of tanshinones and the pharmacological effects of their active ingredients. *Front. Pharmacol.* **11**, 193 (2020).
17. Wang, D. *et al.* A tanshinone I derivative enhances the activities of antibiotics against Staphylococcus aureus in vitro and in vivo. *Res. Microbiol.* **168**, 46–54 (2017).
18. Zhou, X. *et al.* Danshensu is the major marker for the antioxidant and vasorelaxation effects of Danshen (Salvia miltiorrhiza) water-extracts produced by different heat water-extractions. *Phytomed. Int. J. Phytother. Phytopharmacol.* **19**, 1263–1269 (2012).
19. Zhou, G. J. *et al.* Post-harvest induced production of salvianolic acids and significant promotion of antioxidant properties in roots of Salvia miltiorrhiza (Danshen). *Molecules (Basel, Switzerland)*. **19**, 7207–7222 (2014).
20. Liu, X. *et al.* Salvianolic acids from antithrombotic Traditional Chinese Medicine Danshen are antagonists of human P2Y(1) and P2Y(12) receptors. *Sci. Rep.* **8**, 8084 (2018).
21. Teng, F. *et al.* Salvianolic acid A inhibits endothelial dysfunction and vascular remodeling in spontaneously hypertensive rats. *Life Sci.* **144**, 86–93 (2016).
22. Wang, S. *et al.* Comparison of chemical constituents in scrophulariae radix processed by different methods based on UFLC-MS combined with multivariate statistical analysis. *J. Chromatogr. Sci.* **56**, 122–130 (2018).
23. Duan, J., Su, S., Lv, J., Yan, H. & Ding, A. Traditional experiences and modern cognition on primary processing of traditional Chinese medicinal materials. *China J. Chin. Mater. Med.* **34**, 3151–3157 (2009).
24. Yang, J. J. *et al.* Modern research progress on integration of habitat processing and processing of traditional Chinese medicinal materials. *Chin. Trad. Herbal Drugs*. **49**, 4726–4730 (2018).
25. Du, W. F., Cong, X. D. & Cai, B. C. Study advance on the “sweating” primary processing method of Chinese Medicinal Materials. *Chin Arch. Trad. Chin. Med.* **31**, 341–342 (2013).
26. Chen, R. *et al.* Modern research progress of Chinese materia medica diaphoretic processing method. *Chin. Trad. Herbal Drugs*. **49**, 489–493 (2018).
27. Duan, J. A. *et al.* “Sweating” of traditional Chinese medicinal materials during primary processing and its mechanisms of enzymatic reaction and chemical conversion. *Chin. Trad. Herbal Drugs* **44**, 1219–1225 (2013).
28. Li, G. Z. Comparative study on the effects of sweated and non-sweated Salvia miltiorrhiza on cytochrome P450 isozymes in rats. *Anhui Univ. Chin. Med.* (2018).
29. Yu, F. Comparative study on fingerprint and preliminary Pharmacodynamics of sweated and non-sweated Salvia miltiorrhiza in Vivo and in Vitro. *Anhui Univ. Chin. Med.* (2017).
30. Liang, W. *et al.* Quality evaluation and chemical markers screening of Salvia miltiorrhiza Bge. (Danshen) based on HPLC fingerprints and HPLC-MS(n) coupled with chemometrics. *Mol. (Basel, Switzerland)* **22**, 478 (2017).
31. Liu, X., Wu, Z., Yang, K., Ding, H. & Wu, Y. Quantitative analysis combined with chromatographic fingerprint for comprehensive evaluation of Danhong injection using HPLC-DAD. *J. Pharm. Biomed. Anal.* **76**, 70–74 (2013).
32. Wolfender, J. L., Rudaz, S., Choi, Y. H. & Kim, H. K. Plant metabolomics: from holistic data to relevant biomarkers. *Curr. Med. Chem.* **20**, 1056–1090 (2013).
33. Zhang, Q. *et al.* Guizhi-Shaoyao-Zhimu decoction possesses anti-arthritis effects on type II collagen-induced arthritis in rats via suppression of inflammatory reactions, inhibition of invasion & migration and induction of apoptosis in synovial fibroblasts. *Biomed. Pharmacother.* **118**, 109367 (2019).
34. Lu, X. *et al.* LC-MS-based metabolomics analysis. *J. Chromatogr. B Anal. Technol. Biomed. Life Sci.* **866**, 64–76 (2008).
35. Raman, M. *et al.* Parenteral nutrition and lipids. *Nutrients*. **9**, 388 (2017).
36. Fiorito, S., Epifano, F., Preziuso, F., Taddeo, V. A. & Genovese, S. Biomolecular targets of oxyprenylated phenylpropanoids and polyketides. *Prog. Chem. Org. Nat. Prod.* **108**, 143–205 (2019).
37. Chen, J. J., Lin, W. J., Liao, C. H. & Shieh, P. C. Anti-inflammatory benzenoids from Antrodia camphorata. *J. Nat. Prod.* **70**, 989 (2007).
38. Kanehisa, M. Toward understanding the origin and evolution of cellular organisms. *Protein Sci.* **28**, 1947–1951 (2019).
39. Bellissimo, M. P. *et al.* Plasma high-resolution metabolomics identifies linoleic acid and linked metabolic pathways associated with bone mineral density. *Clinical nutrition (Edinburgh, Scotland)*. <https://doi.org/10.1016/j.clnu.2020.05.041>, (2020)..
40. Salari-Moghaddam, A., Naghshi, S., Larijani, B. & Esmailzadeh, A. The protective association of linoleic acid against mortality might be under- or over-estimated. *Am. J. Clin. Nutr.* **112**, 237–237 (2020).
41. Mądry, E. *et al.* Body fat changes and liver safety in obese and overweight women supplemented with conjugated linoleic acid: a 12-week randomised, double-blind. *Placebo Control. Trial. Nutr.* **12**, 1811 (2020).
42. Sun, C. *et al.* Salvia miltiorrhiza stem-leaf active components of salvianolic acids and flavonoids improved the hemorheological disorder and vascular endothelial function on microcirculation dysfunction rats. *Phytother. Res.* **34**, 1704–1720 (2020).
43. Shi, K. *et al.* Identification and functional analyses of differentially expressed metabolites in early stage endometrial carcinoma. *Cancer Sci.* **109**, 1032–1043 (2018).

44. Behera, B. C., Mahadik, N. & Morey, M. Antioxidative and cardiovascular-protective activities of metabolite usnic acid and psomic acid produced by lichen species *Usnea complanata* under submerged fermentation. *Pharm. Biol.* **50**, 968–979 (2012).
45. Li, G. *et al.* Comparison of the chromatographic fingerprint, multicomponent quantitation and antioxidant activity of *Salvia miltiorrhiza* Bge. between sweating and nonsweating. *Biomed. Chromatogr.* **32**, 4203 (2018).
46. Yu, F. *et al.* Influence of different sweating conditions on the content of tanshinones in *salvia miltiorrhiza*. *Anhui Univ. Chin. MED.* **36**, 73–77 (2017).
47. Rischer, H. *et al.* Gene-to-metabolite networks for terpenoid indole alkaloid biosynthesis in *Catharanthus roseus* cells. *Proc. Natl. Acad. Sci.* **103**, 5614–5619 (2006).
48. Xie, C. L. *et al.* Mapping the metabolic signatures of fermentation broth, mycelium, fruiting body and spores powder from *Ganoderma lucidum* by untargeted metabolomics. *LWT Food Sci. Technol.* **19**, 109494 (2020).
49. Bhandari, S. *et al.* Pleiotropic effects of statins in hypercholesterolaemia: a prospective observational study using a lipoproteomic based approach. *Lancet*. null: S21 (2015).
50. Lauren, H. *et al.* Untargeted metabolomic screen reveals changes in human plasma metabolite profiles following consumption of fresh broccoli sprouts. *Mol. Nutr. Food Res.* **62**, e1700665 (2018).
51. Rizvi, N. F., Weaver, J. D., Cram, E. J., Lee-Parsons, C. W. T. & Sangeeta, D. Silencing the transcriptional repressor, ZCT1, illustrates the tight regulation of terpenoid indole alkaloid biosynthesis in *catharanthus roseus* hairy roots. *PLoS ONE* **11**, e0159712 (2016).
52. Li, X. L. *et al.* LC-MS-based metabolomic approach revealed the significantly different metabolic profiles of five commercial truffle species. *Front. Microbiol.* **10**, 02227 (2019).
53. Vranova, E., Coman, D. & Gruißsem, W. Network analysis of the MVA and MEP pathways for isoprenoid synthesis. *Annu. Rev. Plant Biol.* **64**, 665–700 (2013).

Acknowledgements

We would like to thank Dr. Qifang Pan and Qian Shen from Shanghai Jiaotong University for helping to revise the manuscript. We also thank Shanghai OE Biotech Co., Ltd for metabolomics analysis. We thank Prof. Biao Cai and Jimin Zhu from College of Integrated Chinese and Western medicine, Anhui University of Chinese Medicine for helpful comments on the specific pharmacological actions of differential metabolites and statistical analysis, respectively.

Authors contributions

S.X., M.C., D.P.: Conceived, designed, and implemented the study; M.C., S.X., W.J.: Statistics analysis; S.X., D.P., Y.L. and W.C.: Reagents/materials/analysis tools; X.S., M.C., X.M.: Drafted the manuscript; All authors edited the manuscript and approved the final version.

Funding

This work was supported by the NSF of Anhui Province (Grant No. 1908085MH268), Key Natural Science Research Projects in Anhui Universities (Grant No. KJ2019A0453), Returnee Program of Anhui People's Society Office (Grant No. DT18100035) and Key Project of Scientific Research Fund of Anhui University of Traditional Chinese Medicine (Grant No. 2018zrzd05).

Competing interests

The authors declare no competing interests.

Additional information

Supplementary information is available for this paper at <https://doi.org/10.1038/s41598-020-76650-w>.

Correspondence and requests for materials should be addressed to S.X.

Reprints and permissions information is available at www.nature.com/reprints.

Publisher's note Springer Nature remains neutral with regard to jurisdictional claims in published maps and institutional affiliations.



Open Access This article is licensed under a Creative Commons Attribution 4.0 International License, which permits use, sharing, adaptation, distribution and reproduction in any medium or format, as long as you give appropriate credit to the original author(s) and the source, provide a link to the Creative Commons licence, and indicate if changes were made. The images or other third party material in this article are included in the article's Creative Commons licence, unless indicated otherwise in a credit line to the material. If material is not included in the article's Creative Commons licence and your intended use is not permitted by statutory regulation or exceeds the permitted use, you will need to obtain permission directly from the copyright holder. To view a copy of this licence, visit <http://creativecommons.org/licenses/by/4.0/>.

© The Author(s) 2020